

Measurement of Cytosolic Calcium Using ^{19}F NMR

by Elizabeth Murphy,* Louis Levy,* Bore Raju,* Charles Steenbergen,[†] John T. Gerig,[‡] Phirtu Singh,[§] and Robert E. London*

Fluorine-19 nuclear magnetic resonance (NMR) studies of cells and perfused organs loaded with fluorinated ion chelators represent a new approach to determining cytosolic free calcium levels *in situ*. The molecular basis for this approach and the relative advantages and disadvantages of the NMR technique are discussed in this paper. Results obtained on perfused normoxic and ischemic rat hearts are presented, indicating that ischemia is associated with an elevation in the level of cytosolic free calcium before the onset of irreversible cell injury. The results are therefore consistent with this elevation playing a causative role in the mediation of myocardial cell injury resulting from ischemia.

Introduction

As discussed elsewhere (1,2) cytosolic free calcium $[\text{Ca}^{2+}]_i$ is an important regulator of cell physiology, and perturbations of $[\text{Ca}^{2+}]_i$ may be important in mediating cell injury resulting from chemical or physical agents. Accurate methods for the measurement of $[\text{Ca}^{2+}]_i$ and other ions are central to elucidating the role of ions in these processes. Many of the methods used for making such measurements involve the introduction of chelators into the cytosol so that changes in $[\text{Ca}^{2+}]_i$ can be followed by the corresponding spectral changes that accompany calcium-chelator complexation. Several types of $[\text{Ca}^{2+}]_i$ indicators including fluorescent chelators (3), photoproteins (4), and metallochromic dyes (5) have been used to measure $[\text{Ca}^{2+}]_i$. Recently, nuclear magnetic resonance (NMR) measurements of $[\text{Ca}^{2+}]_i$ levels have been made, based on the analogous introduction of fluorinated calcium chelators into cells (6-8). This manuscript discusses in detail the ^{19}F NMR methods for measuring $[\text{Ca}^{2+}]_i$, as well as related ^{19}F NMR

methods for measuring $[\text{Mg}]_i$. In addition, the usefulness of these methods is illustrated in a series of experiments showing that an increase in $[\text{Ca}^{2+}]_i$ precedes lethal myocardial cell injury during ischemia.

Materials and Methods

Adult, male Sprague-Dawley rats weighing 200 to 300 g were anesthetized with pentobarbital. The heart was excised and the aorta was cannulated within 15 sec. Retrograde perfusion was started from a reservoir 90 cm above the aortic cannula. The perfusate was Krebs-Henseleit buffer containing 120 mM NaCl, 4.7 mM KCl, 1.2 mM MgSO_4 , 1.2 mM KH_2PO_4 , 1.25 mM CaCl_2 , 25 mM NaHCO_3 , and 10 mM glucose. The buffer was continuously aerated with humidified 95% O_2 and 5% CO_2 and was maintained at 37°C.

For assessment of contractile function, a rubber balloon on the tip of a polyethylene catheter was inserted through the left atrium into the left ventricle. The catheter was connected to a Statham P23d pressure transducer that was outside the magnet located at the same height as the heart. The balloon was inflated to give an end-diastolic pressure of 5 to 15 cm of water.

After 15 min of control, nonrecirculating perfusion, the heart was perfused with 150 to 400 mL of a Krebs-Henseleit solution containing 5 μM of the acetoxymethyl ester of the appropriate ^{19}F NMR indicator. After the indicator loading was completed, the heart was placed in a standard 20-mm NMR tube with the

*Laboratory of Molecular Biophysics, National Institute of Environmental Health Sciences, Research Triangle Park, NC 27709.

[†]Department of Pathology, Duke University Medical Center, Durham, NC 27706.

[‡]Department of Chemistry, University of California, Santa Barbara, Santa Barbara, CA 93106.

[§]Department of Chemistry, North Carolina State University, Raleigh, NC 27695.

Address reprint requests to E. Murphy, Laboratory of Molecular Biophysics, National Institute of Environmental Health Sciences, Research Triangle Park, NC 27709.

apex of the heart approximately 1 cm from the bottom of the tube. The perfusate was evacuated by PE tubing connected to a variable speed Masterflex peristaltic pump that extended to the bottom of the tube.

NMR studies were performed on a Nicolet NT 360 NMR spectrometer at 37°C, using either a 20 mm ^{19}F probe tuned to 339.7 MHz (Doty Scientific, Columbia, SC) or a 20-mm broad-band Nicolet probe with decoupler tuned to 339.7 MHz for the ^{19}F studies and the observe coil tuned to ^{31}P . The sample was shimmed on H_2O , and we routinely obtained a (non-spinning) line width at half height of approximately 0.25 ppm. For the ^{19}F studies we used a 40° pulse angle, a 500 μs delay, and 127 ms acquisition time. A 70° pulse angle, a 1-sec delay, and a 205-msec acquisition time were used for the ^{31}P studies.

Results and Discussion

The calcium chelator, 5FBAPTA is introduced into cells and perfused organs as the acetoxymethylester (AME), a form that is readily permeable across the plasma membrane (9). Once inside the cell, naturally occurring esterases cleave the AME, leaving the negatively charged 5FBAPTA trapped in the cytosol. The 5FBAPTA undergoes an NMR chemical shift upon binding calcium, the basis for which is apparent from the X-ray crystal structure (10). The chelator 5FBAPTA forms an octadentate complex with calcium ions, as illustrated in Figure 1. This complex involves the coordination of one of the carboxyl oxygen atoms from each of the four carboxyl groups, the two ether oxygen atoms, and the two anilinic nitrogen atoms. The formation of a nearly tetrahedral, sp^3 bonding structure for the nitrogens alters the conjugation with the aromatic system and is responsible for the large perturbation of the ^{19}F chemical shift that accompanies complexation. As discussed by Tsien (3), analogous structural changes accompanying calcium ion complexation with the fluorescent indicators can provide the basis for the observed spectral changes as well.

The ^{19}F NMR spectrum of 5FBAPTA in the presence of a nonsaturating level of calcium exhibits two resonances corresponding to the uncomplexed and to the calcium complexed species (Fig. 2). The simultaneous observation of both resonances reflects the fact that the rate of dissociation of the calcium-chelator complex falls into the slow exchange limit in which the lifetime of the Ca-5FBAPTA complex is longer than the reciprocal of the chemical shift difference ($\text{GK } \tau > 1/\delta \text{ ppm} = 4.9 \times 10^{-4} \text{ sec}$). As illustrated in Figure 2, the observation of the two ^{19}F resonances, coupled with a knowledge of the calcium dissociation constant, allows a determination of the $[\text{Ca}^{2+}]$ value. The reported values for the dissociation constant of Ca-FBAPTA have ranged from 285 nM measured at 30°C, pH 7.2 (no Mg) (11); to 337 nM at 37°C, pH 7.2 (no Mg) (11); to 451 nM at 30°C, pH 7.1 (0.5 mM Mg) (12); to 635 nM at 37°C, pH 7.05 (no Mg) (8); to 708 nM

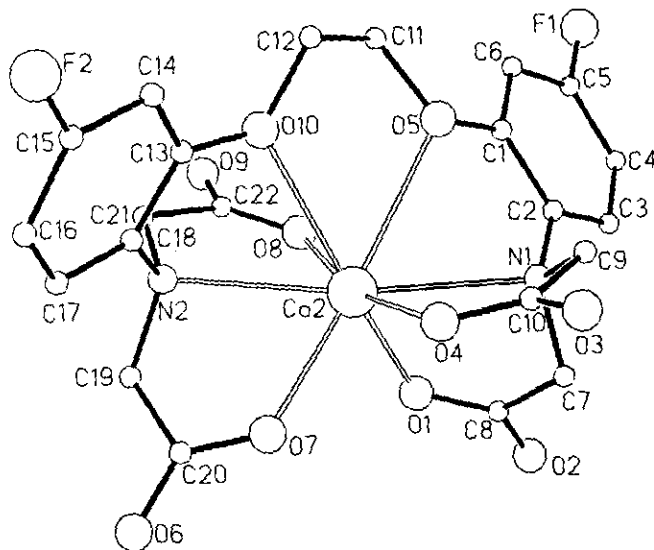
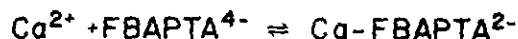


FIGURE 1. Ligand geometry of $\text{Ca}(\text{CaFBAPTA}) \cdot 5\text{H}_2\text{O}$. Calcium is octocoordinated with a single FBAPTA molecule.

at 37°C, pH 7.1 (no Mg) (6). These measurements illustrate the trend of higher K_d values associated with increased temperature. However, the discrepancies are currently somewhat larger than expected and further work is necessary to arrive at a consensus value.

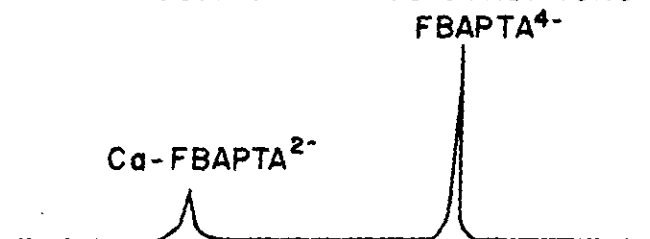
The K_d values are measured in model solutions made to approximate the intracellular milieu. To better define the intracellular ionic environment, we

CHELATE EQUILIBRIUM:



$$K_D = \frac{[\text{Ca}^{2+}][\text{FBAPTA}^{4-}]}{[\text{Ca-FBAPTA}^{2-}]}$$

FOR SLOW EXCHANGE CONDITIONS:



$$[\text{Ca}^{2+}] = K_D \frac{[\text{Ca-FBAPTA}^{2-}]}{[\text{FBAPTA}^{4-}]}$$

FIGURE 2. Calculation of $[\text{Ca}^{2+}]$ from the ^{19}F NMR resonances of FBAPTA in slow exchange with calcium.

recently developed a fluorinated magnesium ion indicator (13). Just as the EGTA molecule forms a useful starting point for the development of calcium-sensitive indicators (3), the development of magnesium-sensitive indicators has proceeded by modifying the structure of EDTA. Specifically, the replacement of the central ethylene moiety by a fluorinated benzene, and the substitution of one of the *N,N* diacetic acid groups with an oxoacetic acid, results in a fluorinated *O*-aminophenol-*N,N,O*-triacetate (APTRA) structure, which we have found useful for carrying out intracellular magnesium ion measurements. These molecules exhibit magnesium K_d values that are closely matched to the anticipated cytosolic magnesium concentrations. Although the calcium K_d values are somewhat lower, they are still 100- to 1000-fold greater than typical cytosolic calcium values. With the possible exception of extreme pathological states, the presence of calcium will not interfere with the magnesium determination. For two of the fluorinated derivatives studied, 5-fluoro APTRA and 4-methyl, 5-fluoro APTRA, the kinetics of the magnesium chelator interaction again fall into the slow exchange limit at the field strength used in this study. Therefore, two resonances can be observed, and the level of magnesium determined is analogous to the calcium determination illustrated in Figure 2. Finally, it is worth noting that the APTRA structure readily lends itself to further modification to include fluorophores analogous to those utilized for intracellular calcium ion indicators (14). Cytosolic free magnesium levels measured with 5FAPTRA in perfused rat heart average 0.85 mM.

The relative advantages and disadvantages of the use of NMR-sensitive indicators are summarized in Table 1. Briefly, the absence of fluorine-containing metabolites in the cell makes it possible to carry out

^{19}F NMR measurements with no observable background. This contrast with optical indicators must contend with optical background and interference from other chromophores such as hemoglobin and NADH, as well as motion artifacts. Furthermore, this NMR spectral technique measures the signal of the entire perfused organ and is not restricted to obtaining data from only the surface layer of cells, as is the case with optical techniques. In addition, the possibility of observing separate, resolvable resonances for different ions eliminates confusion that might arise from the presence of other trace ions that bind with high affinity to the indicator. Finally, the ability to determine the $[\text{Ca}^{2+}]_i$ level, based on a direct observation of the two resonances corresponding to uncomplexed and calcium-complexed indicator, allows the measurement of $[\text{Ca}^{2+}]_i$ independent of the concentration of the indicator.

There are, however, several drawbacks to the ^{19}F NMR determinations of $[\text{Ca}^{2+}]_i$ levels. In particular, NMR is an inherently insensitive technique and, thus, requires large concentrations of cells and frequently higher concentrations of the intracellular chelator than do the optical methods. As a consequence of this inherent insensitivity, signal averaging becomes essential; hence, the time resolution for the NMR determination is considerably slower (min) than for most optical methods (msec to sec).

In summary, ^{19}F NMR is the method of choice for monitoring $[\text{Ca}^{2+}]_i$ under the following conditions: *a*) studies of systems with a significant optical background or interference, such as red blood cells; *b*) studies of perfused organs, in which $[\text{Ca}^{2+}]_i$ needs to be measured throughout the entire organ; and *c*) studies under conditions in which significant levels of interfering ions are present.

This ^{19}F NMR method has proved useful in studying the involvement of calcium in lethal myocardial cell injury (15). Several investigators (2,16) have suggested a role for calcium in lethal myocardial cell injury produced by ischemia. If an elevation in $[\text{Ca}^{2+}]_i$ is responsible for lethal cell injury, then an increase in $[\text{Ca}^{2+}]_i$ prior to the onset of lethal cell injury is a necessary condition. This question can be ideally addressed using ^{19}F NMR studies of 5FBAPTA-loaded perfused hearts.

Figure 3 shows ^{19}F NMR spectra of a perfused rat heart loaded with 5FBAPTA. Since no attempt was made to gate the pulses to the cardiac cycle, the results correspond to a time average of the $[\text{Ca}^{2+}]_i$ concentration over the entire cardiac cycle. The basal (preischemic), time-average intensity ratio of Ca-FBAPTA/FBAPTA for 10 such spectra was 0.9, giving a calculated $[\text{Ca}^{2+}]_i$ value of 630 ± 97 nM. An estimate of the diastolic calcium concentration obtained by arresting the heart with 15 mM MgCl_2 , was 180 ± 28 nM.

Hearts globally ischemic for 15 min showed a 3-fold rise in $[\text{Ca}^{2+}]_i$ above the basal time average $[\text{Ca}^{2+}]_i$ (Fig. 3). Following 10 to 15 min of reperfusion, the

Table 1. Advantages and disadvantages of ^{19}F NMR calcium chelators.

Advantages	
No background or optical interference	
• No interference from endogenous chromophores	
The NMR signal is from all the tissue in the coil	
• Allows measurements in perfused organs and animals	
Separate resonance peaks for Ca-FBAPTA and FBAPTA	
• $[\text{Ca}^{2+}]_i$ measurements are independent of indicator concentration trace metals (e.g., Zn) also give separate resonances	
Disadvantages	
Poor sensitivity	
• Requires large amounts of cells and tissues and/or higher concentrations of intracellular indicator	
• Requires signal averaging over minutes, resulting in poor time resolution	
Summary	
^{19}F NMR indicators are the method of choice for	
• Red blood cells	
• Perfused organs	
• Cells in the presence of interfering ions	

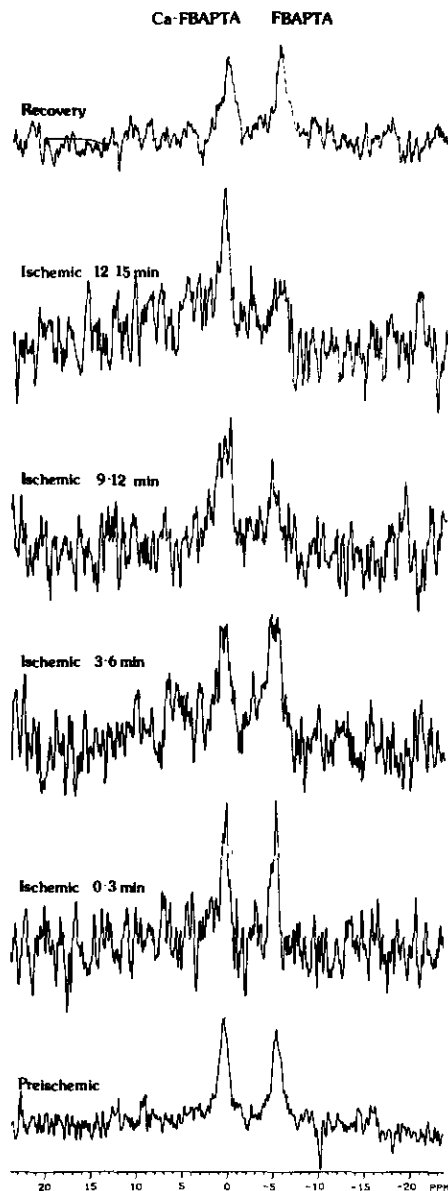


FIGURE 3. ^{19}F NMR spectra of 5FBAPTA-loaded perfused rat heart.

heart resumed beating, $[\text{Ca}^{2+}]_i$ returned to basal level, and there was no detectable loss of 5FBAPTA from the heart. In addition, ^{31}P -NMR measurements showed that upon reperfusion, creatine phosphate was restored to its preischemic level. If we define lethal myocardial cell injury as *a*) an immediate loss during reperfusion of intracellular components, such as the enzyme lactate dehydrogenase or the intracellular indicator 5FBAPTA, *b*) a loss of creatine from the cell such that creatine phosphate does not return to its preischemic level during reperfusion, and *c*) a loss of the capacity to resynthesize ATP, then the rise in $[\text{Ca}^{2+}]_i$ is clearly seen to precede the development of irreversible injury. Hence, the results are consistent with the interpretation that an elevation in $[\text{Ca}^{2+}]_i$ may play a causative role in the production of irreversible cell injury.

Using this ^{19}F NMR approach, we can further show that manipulations that delay the rise in $[\text{Ca}^{2+}]_i$ also delay the onset of lethal injury. Arresting the heart with 15 mM magnesium prior to ischemia has been reported to delay the development of ischemic injury. Even though magnesium arrest delays the increase in $[\text{Ca}^{2+}]_i$, the myocytes eventually attain a level of $[\text{Ca}^{2+}]_i$ comparable to that in hearts that were beating prior to ischemia; in both cases, the increase in $[\text{Ca}^{2+}]_i$ occurs before the onset of irreversible injury as defined above. These data are consistent with the hypothesis that an increased $[\text{Ca}^{2+}]_i$ is in the onset of lethal cell injury.

C. S. supported by NIH grants HL39752 and HL01337.

REFERENCES

1. Rasmussen, H., and Barrett, P. Q. Calcium messenger system: an integrated view. *Physiol. Rev.* 64: 938-984 (1984).
2. Farber, J. L. *Biology of disease: membrane injury and calcium homeostasis in the pathogenesis of coagulative necrosis*. Lab Invest. 47: 114-123 (1982).
3. Tsien, R. Y. New calcium indicators and buffers with high selectivity against magnesium and protons: design, synthesis, and properties of prototype structures. *Biochemistry* 19: 2396-2404 (1980).
4. Blinks, J. R., Prendergast, F. G., and Allen, D. G. Photoproteins as biological calcium indicators. *Pharmac. Rev.* 28: 1-93 (1976).
5. Scarpa, A., Brinley, F. J., and Dubyak, G. Antipyrylazo III: a middle range calcium metallochromic indicator. *Biochemistry* 17: 1378-1386 (1978).
6. Smith, G. A., Hesketh, R. T., Metcalfe, J. C., Feeney, J., and Morris, P. G. Intracellular calcium measurements by ^{19}F NMR of fluorine-labeled chelators. *Proc. Natl. Acad. Sci. (U.S.A.)* 80: 7178-7182 (1983).
7. Murphy, E., Levy, L., Berkowitz, L. R., Orringer, E. P., Gabel, S. A., and London, R. E. Nuclear magnetic resonance measurement of cytosolic free calcium levels in human red blood cells. *Am. J. Physiol.* 251: C496-C504 (1986).
8. Levy, L., Murphy, E., and London, R. E. Synthesis and characterization of ^{19}F NMR chelators for measurement of cytosolic free Ca. *Am. J. Physiol.* 252: C441-C449 (1987).
9. Tsien, R. Y. A non-disruptive technique for loading calcium buffers and indicators into cells. *Nature* 290: 527-528 (1981).
10. Gerig, J. T., Singh, P., Levy, L., and London, R. E. Calcium complexation with a highly calcium selective chelator: crystal structure of $\text{Ca}(\text{caFBAPTA}) \cdot 5\text{H}_2\text{O}$. *J. Inorganic Biochem.* 31: 113-121 (1987).
11. Marban, E., Kitakaze, M., Kusuoka, H., Porterfield, J. K., Yue, D. T., and Chacko, V. P. Intracellular free calcium concentration measured with ^{19}F NMR spectroscopy in intact ferret hearts. *Proc. Natl. Acad. Sci. (U.S.A.)* 84: 6005-6009 (1987).
12. Schanne, F. A. X., Gupta, R. K., and Rosen, J. F. ^{19}F NMR detection of the effects of lead toxicity on intracellular $[\text{Ca}^{2+}]_i$ in osteoblastic bone cells. *Biophys. J.* 53: 215a (1988).
13. Levy, L., Murphy, E., Raju, B., and London, R. E. Measurement of cytosolic free magnesium concentration by ^{19}F NMR. *Biochemistry* 27: 4041-4048 (1988).
14. Grynkiewicz, G., Poenie, M., and Tsien, R. Y. A new generation of $[\text{Ca}^{2+}]_i$ indicators with greatly improved fluorescence properties. *J. Biol. Chem.* 260: 3440-3450 (1985).
15. Steenbergen, C., Murphy, E., Levy, L., and London, R. E. Elevation in cytosolic free calcium concentration early in myocardial ischemia in perfused rat heart. *Circ. Res.* 60: 700-707 (1987).
16. Nayler, W. G. The role of calcium in the ischemic myocardium. *Am. J. Pathol.* 102: 262-272 (1981).